Bandwidth and Fermi surface of iron oxypnictides: Covalency and sensitivity to structural changes

Verónica Vildosola,[1,2,3] Leonid Pourovskii,[1] Ryotaro Arita,[3,4] Silke Biermann,[1,3] and Antoine Georges[1,3]
[1]*Centre de Physique Théorique, École Polytechnique, CNRS, 91128 Palaiseau, France*
[2]*Departamento de Física, Comisión Nacional de Energía Atómica (CNEA)-CONICET, San Martín, Provincia de Buenos Aires, Argentina*
[3]*Japan Science and Technology Agency, CREST, Japan*
[4]*Department of Applied Physics, University of Tokyo, Tokyo 113-8656, Japan*
(Received 20 June 2008; revised manuscript received 21 July 2008; published 27 August 2008)

Some important aspects of the electronic structure of the iron oxypnictides depend very sensitively on small changes in interatomic distances and bond angles within the iron-pnictogen subunit. Using first-principles full-potential electronic structure calculations, we investigate this sensitive dependence, contrasting in particular LaFeAsO and LaFePO. The width of the Fe bands is significantly larger for LaFePO, indicating a better metal and weaker electronic correlations. When calculated at their experimental crystal structures, these two materials have significantly different low-energy band structures. The topology of the Fermi surface changes when going from LaFePO to LaFeAsO, with a three-dimensional hole pocket present in the former case transforming into a tube with two-dimensional dispersion. We show that the low-energy band structure of LaFeAsO evolves toward that of LaFePO as the As atom is lowered closer to the Fe plane with respect to its experimental position. The physical origin of this sensitivity to the iron-pnictogen distance is the covalency of the iron-pnictogen bond, leading to strong hybridization effects. To illustrate this, we construct Wannier functions, which are found to have a large spatial extension when the energy window is restricted to the bands with dominant iron character. Finally, we show that the Fe bandwidth slightly increases as one moves along the rare-earth series in REFeAsO and we discuss the physical origin of this effect.

DOI: 10.1103/PhysRevB.78.064518 PACS number(s): 74.25.Jb, 74.70.Dd

I. INTRODUCTION

The recent discovery of superconductivity in electron-doped rare-earth oxyarsenides[1] has generated a great deal of interest in the electronic structure and magnetic properties of these compounds, with different types of magnetic[2,3] or charge[4] fluctuations conjectured to be at the origin of the pairing mechanism.

The rare-earth iron oxyarsenides belong to a wider class of rare-earth oxypnictides RE*T*PnO (where RE and *T* are the rare-earth and transition metals, respectively; Pn=P,As is the pnictogen ion, with a nominal charge of −3), which have the same tetragonal structure of ZrCuSiAs type.[5] In spite of obvious similarities in the overall electronic structure, these compounds differ in their magnetic properties and their tendencies toward superconductivity. It is particularly interesting in this respect to contrast the properties of LaFeAsO with those of its phosphate homolog LaFePO. Relating the observed differences to relevant differences in their electronic structure may provide important clues into the nature and the origin of magnetism and superconductivity in these materials. The undoped stoichiometric compounds have different magnetic properties: LaFePO is nonmagnetic,[6] while LaFeAsO undergoes a magnetic ordering transition at a temperature of 134 K (Ref. 1) preceded by a structural transition at a slightly higher temperature.[7] Their transport properties above the magnetic transition temperatures are also different, with the electrical conductivity of LaFePO being substantially larger than that of LaFeAsO.[1,8] These compounds also differ significantly in their superconducting properties. While undoped LaFeAsO is magnetic and nonsuperconducting, the situation in the absence of doping for the parent compound LaFePO is currently somewhat controversial. A superconducting transition in the range of 4–7 K was originally reported[9] and recently confirmed in Ref. 8 but was questioned in Ref. 10, which found no superconductivity above 0.35 K. At any rate, electron doping suppresses the antiferromagnetism in LaFeAsO and leads to a superconducting phase with T_c as high as 26 K, while it does not induce such drastic changes in the phosphate compound, in which it causes only a moderate increase in T_c of up to 8 K.[8]

The electronic structure of the LaFePO compound, in particular its Fermi surface (FS), was investigated theoretically by Lebègue.[11] His results can be outlined as follows: The LaFePO FS consists of two ellipsoidal electronic cylinders centered at the *M*-*A* line at the Brillouin-zone (BZ) edge and of two hole cylinders centered at the BZ center Γ-*Z* line, together with a single hole pocket with three-dimensional (3D)–like dispersion at the *Z* point. A basically identical shape of the FS has been proposed in several theoretical papers[12–16] for LaFeAsO, with electron doping resulting in the disappearance of the 3D hole pocket, which gets filled, thus changing the FS topology and increasing the two-dimensional character upon doping. This topological change and reduction in effective dimensionality has been suggested to be at the origin of the different types of magnetic fluctuations observed in the stoichometric and doped LaFeAsO compounds, respectively.[3,14] It is possibly also responsible for the appearance of superconductivity in the doped compound. It is important to note, in this respect, that most electronic structure calculations in Refs. 12–16 were carried out at values of the lattice constants and internal parameters (the Fe-As and La-O interplane distances) which were obtained by relaxing the structure within the local-density approxima-

tion (LDA)/generalized gradient approximation (GGA). As pointed out very recently by Mazin *et al.*,[14] rather small changes in the LaFeAsO structural parameters, particularly in the Fe-As interatomic distance, may lead to the disappearance of the 3D hole pocket from the FS of stoichometric LaFeAsO. Furthermore, the internal parameters of the LaFeAsO experimental crystal structure are rather poorly reproduced by theoretical LDA/GGA calculations, with the Fe-As interplane distance being underestimated by about 6%.[17]

For these reasons, a comparative study of the LaFePO and LaFeAsO compounds is especially relevant in order to clarify the relations between the electronic properties and the electronic structures of these materials. We *do know* that stoichometric LaFePO and LaFeAsO differ substantially, particularly in properties directly related to the low-energy electronic structure such as magnetic ordering, transport, and superconductivity. Therefore, one may hope and expect that electronic structure calculations carried out at judiciously chosen structural parameters should be able to capture this difference. In this paper, we carry out a detailed first-principles investigation of LaFeAsO and LaFePO aimed at identifying relevant differences in their electronic structures while relating them to the small but significant differences which exist between the LaFeAsO and LaFePO lattice structures. We show that electronic structure calculations at the *experimental* lattice parameters and internal positions result in the Fermi surfaces of LaFePO and LaFeAsO having different shapes, with the 3D hole pocket present in the case of LaFePO, but not in the case of LaFeAsO. These changes in the FS topology are due to shortening of the iron-pnictogen bond length in LaFePO as compared to that in LaFeAsO. We identify the sensitivity of the electronic structure to this bond length as being due to the rather high degree of covalency associated with the iron-pnictogen bond. We illustrate this point by constructing appropriate Wannier functions.

The paper is organized as follows: We briefly outline our calculational approach in Sec. II. The overall electronic structures of LaFeAsO and LaFePO are discussed in Sec. III. Low-energy aspects of this electronic structure and Fermi surfaces are described in Sec. IV, and the differences between the two materials are illustrated by a study of the sensitivity of these low-energy aspects to the Fe-pnictogen distance. Then, in Sec. V, we perform a Wannier function construction which illustrates this sensitivity and relates it to the covalency of the iron-pnictogen bond. Finally, in Sec. VI we study the influence of the structural properties on the width of the Fe bands and its material dependence.

II. COMPUTATIONAL DETAILS

The first-principles calculations of the band structure and Fermi surface of these materials presented in Secs. III and IV were performed using the full-potential augmented plane wave (APW)+local orbitals method as implemented in the WIEN2K (Ref. 18) code. We considered 800 **k** points in the BZ and checked that all the properties presented in this paper were converged with this mesh. The results that we present here have been obtained within the LDA (Ref. 19) to the exchange-correlation potential. However it is worth mentioning that our conclusions do not vary if we use the GGA (Ref. 20) instead. We have also performed a calculation using the QUANTUM-ESPRESSO package,[21] with the computational details similar to those in Ref. 22, and constructed maximally localized Wannier functions[23] by using the code developed in Ref. 24. Last but not least, we have performed an *N*th-order muffin-tin orbital construction within the atomic spheres approximation (ASA) for the Fe *d* orbitals.[25]

III. BAND STRUCTURES OF LaFeAsO AND LaFePO: COMPARISON ON A LARGE ENERGY SCALE

In this section, we compare the calculated band structures of LaFePO and LaFeAsO at their experimental crystal structures on a large energy scale covering the whole Fe, Pn (=As or P), and O bands as shown in Fig. 1. The crystal structure parameters were taken from experiments and are given in Table I.

The obtained band structures for both materials are depicted in Fig. 1. In this figure, the colors of the bands are simply guides to the eyes in order to compare more easily their relative positions and bandwidths. The bands plotted in (dark gray) red and (light gray) green have mainly Fe 3*d* and Pn-O *p* character, respectively. The bands shown in black correspond mainly to La 4*f* states which are well above the Fe bands. The arrows in between the two plots show the approximate bandwidth of the Fe 3*d* bands in each compound. One may observe that the bands that are close to the Fermi level, which correspond to Fe, have a larger bandwidth in LaFePO as compared to in LaFeAsO. This is a plausible explanation of why the former is observed to be a better metal (in the sense of smaller resistivity).[1,9] This observation is in agreement with previous theoretical reports by Ishibashi *et al.*[26] and also indicates a lesser degree of electronic correlations in LaFePO. It is important to remark that the systems studied in Refs. 1 and 9 were polycrystalline samples and one should be cautious in comparing their resistivity intensities. However, recent photoemission experiments by Lu *et al.*[27] did show a larger bandwidth in LaFePO.

The difference in bandwidth results from a combination of three factors. First, from the difference in Fe-Fe distance, which is significantly smaller in LaFePO. Second, P and As have different electronegativities, which leads to a shift toward more negative energies of the P bands in LaFePO. Finally, Pn has different vertical distances with respect to the Fe plane, a quantity which is mainly governed by the internal *z* parameter, and may influence the width of the Fe's bands through the different strengths of the Fe-Pn bond.

IV. LOW-ENERGY BAND STRUCTURE AND FERMI SURFACE: GREAT SENSITIVITY TO Fe-Pn DISTANCE

In this section, we focus on the very low–energy band structure and Fermi-surface properties of the LaFeAsO and LaFePO compounds, as depicted in Figs. 2 and 3 (calculated for the experimental crystal structure as given in Table I). In both compounds, the Fermi level is crossed by five bands with mainly Fe character. Both materials present two elec-

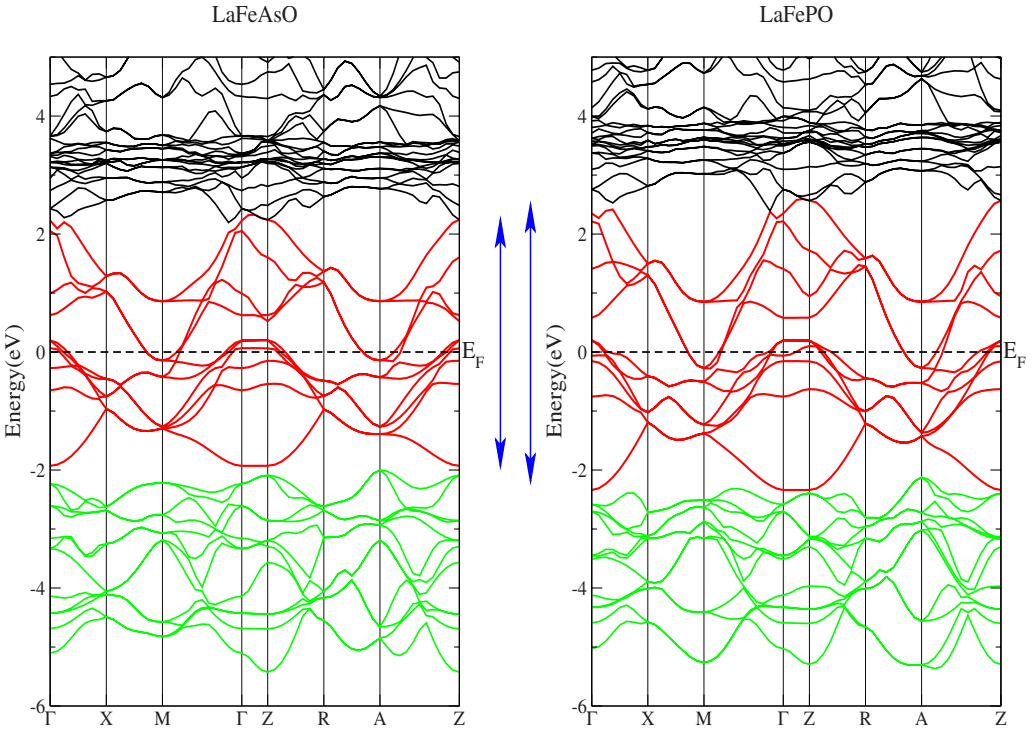

FIG. 1. (Color online) Band structures of LaFeAsO (left) and LaFePO (right). The red (dark gray) and green (light gray) bands have mainly Fe $3d$ and pnictogen/oxygen p characters, respectively. The colors are guides to the eyes in order to facilitate comparison of the relative positions and widths of the bands (see also the arrows).

tron pockets centered at M and two hole pockets centered at Γ with mainly d_{xz} and $d_{xz/yz}$ character. (Our choice of the local coordinate system centered at Fe is such that the x and y axes point toward the nearest-neighbor Fe sites. With this choice, the d_{xy} orbital is the one that points to the Pn atom, while $d_{x^2-y^2}$ points toward the nearest-neighbor Fe.) The significant difference between these compounds comes from the third pocket centered along the $\Gamma \rightarrow Z$ direction. In LaFeAsO this third pocket has mainly d_{xy} character and presents almost no dispersion along the z direction [it is therefore two dimensional (2D) in nature]. In contrast, in LaFePO it consists of a dispersing 3D pocket with mainly $d_{3z^2-r^2}$ character.

This difference in the Fermi surfaces may explain the fact that LaFeAsO is magnetically ordered with better nesting properties than those of LaFePO, for which no magnetic ordering has been reported. When the situation with the superconductivity of undoped LaFePO becomes eventually clarified, this difference in the Fermi surfaces may actually prove to be significant also in this respect.

TABLE I. Crystal-structure data for LaFeAsO (Ref. 7) and LaFePO (Ref. 9). Lattice constants a and c, internal positions of Pn and La(z) in units of c, and the vertical distance of Pn with respect to the Fe plane (d_v). The vertical distance is related to the z parameter by $d_v=(z-0.5)c$ and to the angle θ between the As-Fe bond and the Fe-plane by $\tan(\theta)=(2z-1)c/a$.

	LaFeAsO	LaFePO
a	4.0301 Å	3.9636 Å
c	8.7368 Å	8.5122 Å
z(La)	0.1418	0.1487
z(Pn)	0.6507	0.6339
d_v	1.32 Å	1.14 Å
θ	33.2°	29.9°
$d_{\text{Fe-As}}$	2.41 Å	2.33 Å

The explanation for this difference in the low-energy band structure, as obtained from first-principles electronic structure methods, lies mainly in its great sensitivity to the Fe-Pn distance and to the vertical distance of Pn to the Fe plane. The reason for this sensitivity is that close to the Fermi level, there is a sizable hybridization between Fe and Pn states as will be shown later in detail.

We checked the effect of doping by using the virtual-crystal approximation. We observe that for the experimental structures there are no qualitative changes in the low-energy band structure for LaFeAsO but only a shift of the chemical potential with still three 2D-like pockets crossing the Fermi level. In contrast, for LaFePO, the 3D pocket gets filled and almost disappears from the Fermi surface in the doped compound. One should note that the band structure and FS properties obtained for the *relaxed* LaFeAsO structure (in contrast to the experimental one) using LDA (also reported by Singh and Du[13]) present features that are very similar to the ones described above for the LaFePO material. This is due to the fact that LDA overestimates the Fe-As bonding, so that the Fe-As distance (~2.4 Å experimentally) in the relaxed structure becomes as small as in the LaFePO compound, which is around 2.3 Å. As a result, the LDA relaxed structure of LaFeAsO displays a 3D pocket, which disappears upon doping.

In order to understand better the sensitive dependence of the low-energy band structure on the Pn height with respect

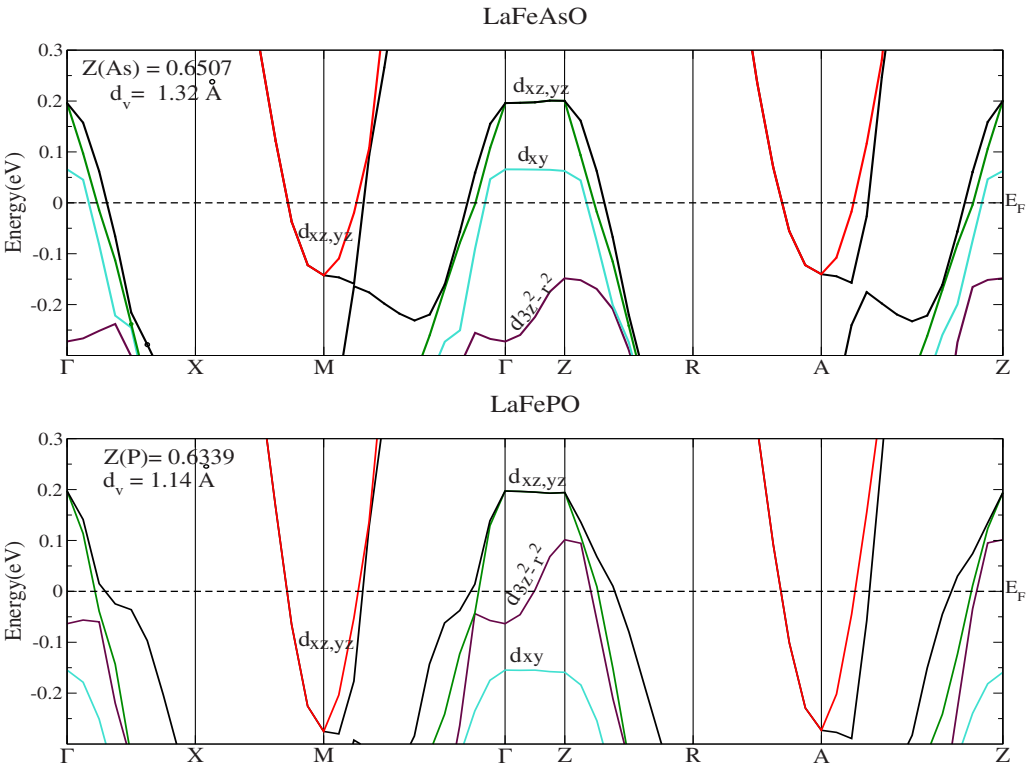

FIG. 2. (Color online) Low-energy region of LaFePnO' s band structures with Pn=As (up panel) and P (lower panel).

to the Fe plane, we have studied the LaFeAsO system by fixing the lattice parameters a and c at their experimental values while varying the vertical position of As all the way from the experimental value down to a position which is very close to the one that P has in the LaFePO material (see Table I). The results of this study are depicted in Fig. 4. We see from this figure that the 2D pocket with d_{xy} character in the "experimental" LaFeAsO (upper panel) evolves into a 3D pocket with $d_{3z^2-r^2}$ character as As is moved closer to the plane (lowest panel). The circles in the plots indicate As contribution (mainly As p_z) to $d_{3z^2-r^2}$. In a nutshell, one can say that LaFeAsO evolves into LaFePO as the height of the As to the Fe plane decreases.

V. ANALYSIS IN TERMS OF WANNIER FUNCTIONS

In Sec. IV we have noted that the low-energy band structure and most notably the topology of the Fermi surface depend very sensitively on the internal structural parameter z(As). Reducing z(As) amounts to decreasing the distance of the As ions to the Fe plane and changing accordingly the angle that the Fe-As bond forms with the Fe plane. In this section, we obtain more direct insights into this sensitive dependence by constructing Wannier functions, which reveal the strong covalency and hybridization effects associated with the Fe-As bond. We present calculations done at the experimental structural parameters.

We have used two different types of Wannier constructions. The first one is a maximally localized Wannier function construction (MLWF) (Ref. 23) based on an ultrasoft pseudopotential approach as implemented in the PWSCF code.[21] The second one is the *N*th-order muffin-tin orbital (NMTO) method and downfolding technique,[25] based on a linear muffin-tin orbital (LMTO)–ASA approach.[28] Previous experience has shown[29] that these two approaches give results that are quite comparable to each other.

A crucial issue is the choice of the energy range on which the downfolding is performed, i.e., the set of Bloch bands that the Wannier construction aims at reproducing. We shall consider two possible choices: a restricted energy range covering roughly $[-2,+2]$ eV around the Fermi level, corresponding to downfolding on the set of $2*5$ bands with domi-

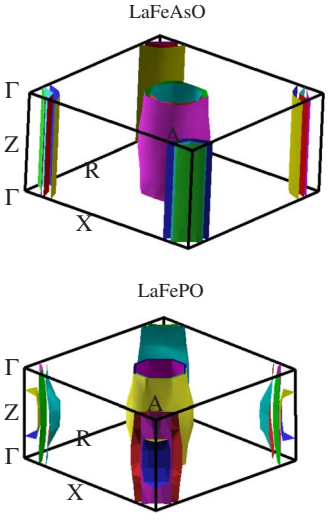

FIG. 3. (Color online) Fermi surfaces for LaFeAsO and LaFePO calculated at their experimental crystal structures.

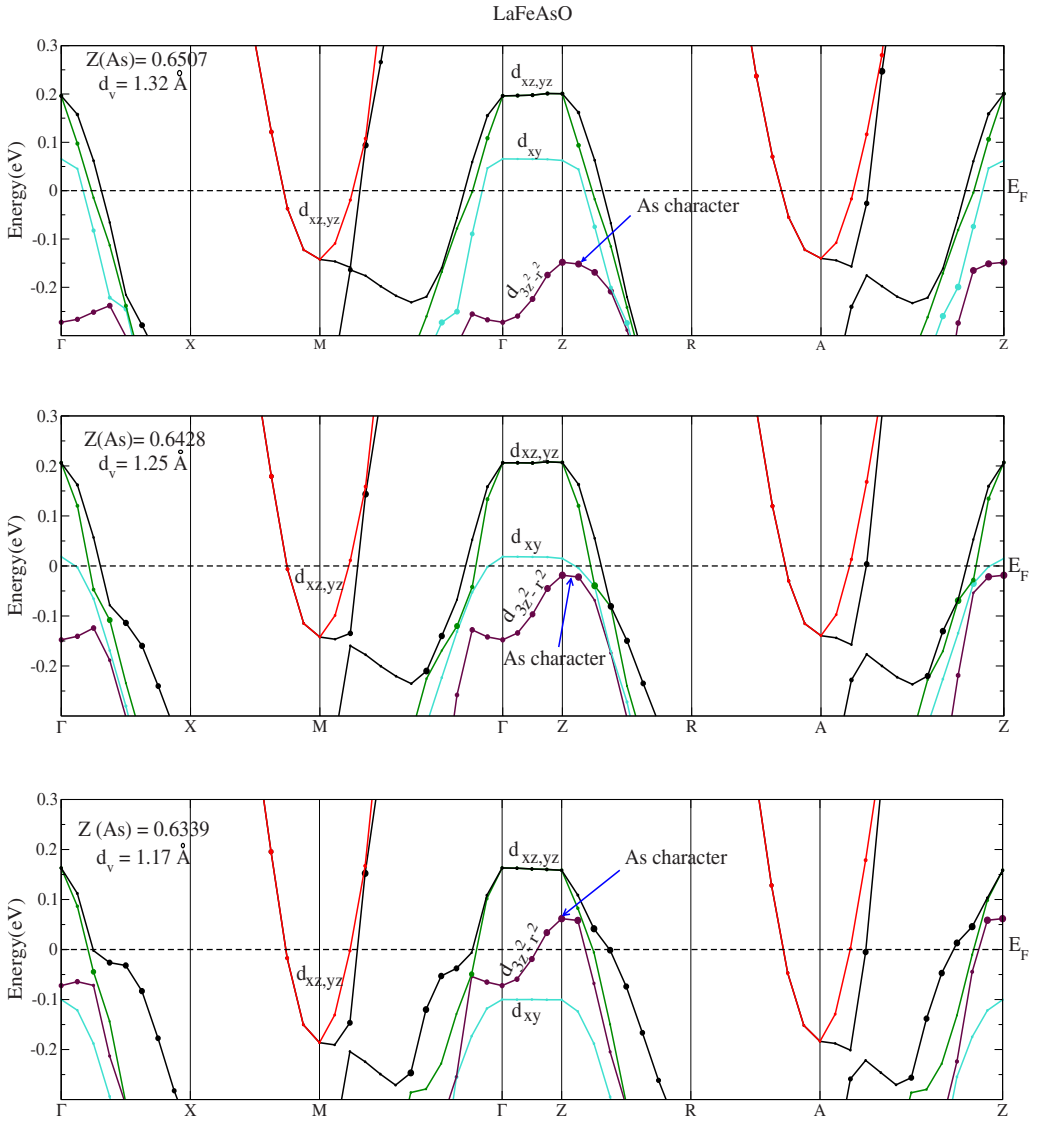

FIG. 4. (Color online) Sensitivity of the low-energy band structure for LaFeAsO to d_v (As's vertical distance with respect to the Fe plane) for fixed lattice constants a and c. The considered d_v values are indicated in each plot.

nant Fe character. We shall call this "d downfolding." We shall also consider downfolding on a much larger energy range (approximately from −6 to +2 eV) encompassing all bands with Fe d, O p, and As p characters ($2*11$ bands), which we shall denote as "dpp downfolding."

In Table II, we display our results for the spatial extension of the various Wannier functions of LaFeAsO obtained by the MLWF construction for both choices of downfolding as measured by the spread $\Omega=\sqrt{(\langle r^2\rangle-\langle r\rangle^2)}$. The most striking feature is the large values of the spreads, in particular of the d_{xy} orbital which points toward the As atoms, when downfolding is performed on the restricted set of Fe bands. Note that the spread of the d_{xy} orbital is actually comparable to the Fe-As distance. The spreads are considerably reduced when performing the dpp downfolding involving the larger set of bands, as expected.

In order to visualize this effect, we plot in Fig. 5(a) the isosurface of the xy-like Wannier function. The "leakage" of the Fe state into the neighboring As atoms is clearly visible. In Fig. 5(b) we plot the same isosurface for the same d_{xy} orbital but in the dpp Wannier construction. As expected, the orbitals are considerably more localized in this case, and the leakage onto the neighboring As atoms is suppressed.

In passing, we note that these observations have direct implications for many-body calculations of these materials performed within the dynamical mean-field theory (DMFT) framework. Because of the spatially extended character of the Fe-Wannier functions in the restricted d downfolding, it seems that including only local matrix elements of the Coulomb interaction and local components of the self-energy would be a rather poor approximation for this "d-only" model. A full model using dpp downfolding (hence with more local Wannier functions) seems like a better starting point for a DMFT calculation. This observation may help in understanding some of the differences recently reported in DMFT calculations of LaFeAsO.[2,30] However, another important issue is the value of the on-site Coulomb interaction and the efficiency of screening, which determines whether

TABLE II. Spreads of maximally localized Wannier functions both for a model retaining only the Fe *d* states and for a model that also includes As and O *p* orbitals. Note in particular the large spread of the *xy* orbital, which points toward the As atom.

Spread (Å)	*d* downfolding	*dpp* downfolding
z^2	1.78	1.02
xz	2.05	1.25
yz	2.05	1.25
xy	2.36	1.24
x^2-y^2	1.73	0.97
As *p*		1.87
As *p*		1.92
As *p*		1.92
O *p*		1.26
O *p*		1.28
O *p*		1.28

these materials should be viewed as in the intermediate or the strong correlation regime.

Finally, in Fig. 6, we display cuts through the isosurfaces of some of the Wannier functions obtained within the NMTO construction within *d* downfolding. More specifically, we have chosen to visualize the most extended orbital (xy), the least extended one (x^2-y^2), and $3z^2-r^2$, which due to its orientation along the z axis plays a special role. Also, as shown in Sec. IV, the roles of the xy and the $3z^2-r^2$ orbitals somewhat interchange concerning the Fermi-surface properties when the z parameter is varied.

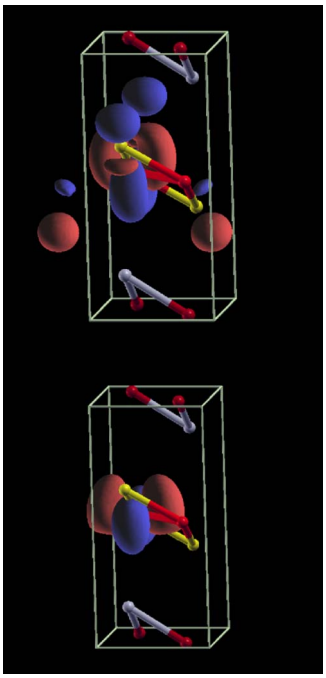

FIG. 5. (Color online) (a) Fe-xy Wannier function for LaFeAsO, from the maximally localized Wannier construction performed for the restricted set of Fe-like bands (*d* downfolding). (b) Same orbital character as in (a) but within the *dpp* downfolding, retaining the full set of Fe *d*, As *p*, and O *p* bands.

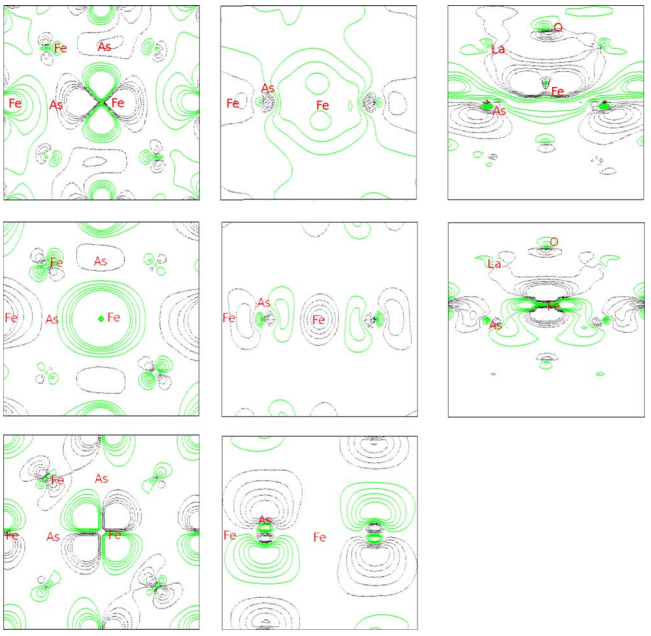

FIG. 6. (Color online) Fe orbitals for the five-band model for LaFeAsO. First row: xy orbital. Second row: $3z^2-r^2$ orbital. Third row: x^2-y^2 orbital. On the Fe plane (first column), on the lower As plane (second column), and on a plane parallel to the z axis containing one La, O, Fe, and As per unit cell (third column). In the first two columns the x axis is along the diagonal of the plots. Note that the x^2-y^2 orbital has nodes on the latter plane and is thus not shown in this representation.

We display three specific cuts: The first two are parallel to the Fe xy plane and correspond to (i) the Fe plane and (ii) a plane containing the lower layer of pnictide atoms. The last one is (iii) a cut along a plane parallel to the z axis and containing a nearest-neighbor Fe-As bond. It thus cuts through half of the La, Fe, O, and As atoms in the unit cell. While the first cut mainly gives the orientation of the Fe orbital, the other two are measures of the leakage of the iron orbitals into the As states. The cuts are represented in the three columns of Fig. 6; the rows show three different Fe *d* orbitals: xy, $3z^2-r^2$, and x^2-y^2.

The first panel in Fig. 6 shows the xy orbital—the one pointing toward the As atoms—of the Fe atom at the center of the plot. Also clearly visible are the contributions of this orbital on the neighboring four Fe atoms, as well as parts of the lobes of the four next-nearest-neighbor Fe atoms. Note, that the two As atoms do not lie on the plane represented here but 1.32 Å above and below. Still, they mediate the hopping to the next-nearest Fe atoms, which display more extended xy character than the nearest neighbors do, consistent with the observation of strong next nearest-neighbor hopping. The second plot in the first row of Fig. 6 shows this same Fe orbital but represented by an isosurface cut containing the As plane. The contributions of the Fe orbital leaking into this plane and in particular onto the two As atoms (eye-like features) are clearly visible. Finally, the cut of this orbital on the plane containing the z axis confirms the very extended nature of this orbital.

The second row of Fig. 6 shows the same cuts but for the $3z^2-r^2$ orbital and the third row those for the x^2-y^2 orbital.

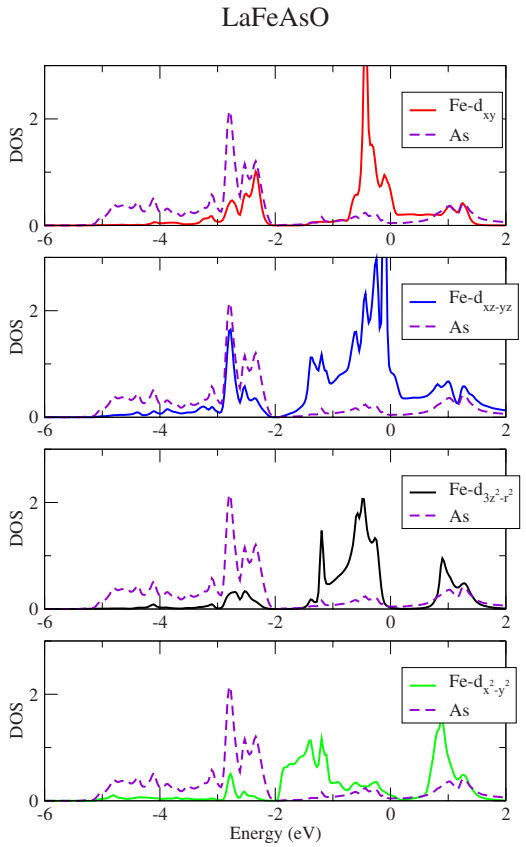

FIG. 7. (Color online) Partial density of states of the Fe d orbitals (solid lines) compared to the As density of states (dashed lines; same curve in all panels).

Particularly interesting are the second plots in these rows, which visualize the hybridization with the $p_x \pm ip_y$ orbitals of the As atoms. For LaFePO (not shown), a similar picture emerges.

The overall comparison of the different orbitals confirms the result in Table I that the xy orbital is by far the most extended one (followed in fact by the yz and xz orbitals—not shown), displaying a tremendous contribution on the neighboring As sites and is in a pancakelike flat shape. Figure 7 shows the partial densities of states (DOSs) of the different Fe d orbitals in comparison with the As partial DOS. The pronounced peaks of the xy and the xz/yz densities of states in the region of the As p bands demonstrate once more that the large spatial extension of these orbitals is due to their hybridizing with the As p states.

The Wannier analysis can thus be summarized by saying that it shows the large extension of the d orbitals when a d downfolding is used, with the xy $(3z^2-r^2)$ being the most (least) extended one. This leakage is consistent with the high sensitivity of the low-energy electronic structure with respect to the z parameter observed in Sec. IV.

VI. WIDTH OF THE IRON BANDS: MATERIALS' DEPENDENCE

Having documented in Secs. II and V (especially from a comparison of LaFePO and LaFeAsO) the importance of covalency and of the Fe-Pn distance, we finally turn to the influence of structural properties on the bandwidth of the iron bands in a broader context. This question has very recently attracted attention, with the observation by Zhao *et al.*[31] of an apparent systematic correlation between the superconducting critical temperature of several different As-based pnictides and the angle formed by the Fe-As bond with respect to the Fe basal plane. Specifically, these authors observed that the various materials under consideration have comparable Fe-As distances (bond lengths) $d_{\text{Fe-As}}$, while the in-plane lattice parameter a decreases as T_c increases. Furthermore, these authors suggested that this may imply a smaller bandwidth W for materials with the highest T_c and hence that superconductivity is enhanced by increasing correlation strength (increasing U/W ratio). Note, however, that this would mean a smaller bandwidth with decreasing Fe-Fe distance.

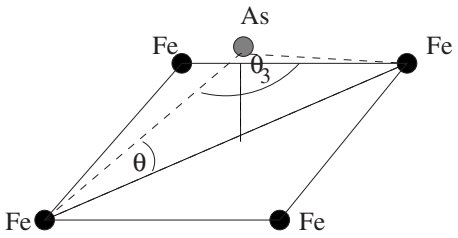

FIG. 8. Schematic Fe_4 As pyramid for LaFeAsO. The θ and θ_3 angles are indicated.

Denoting by θ the angle formed by the Fe-As bond with respect to the basal plane as sketched in Fig. 8 (so that the opening angle at the top of the Fe_4 As pyramid is $\theta_3 = \pi - 2\theta$ in the notations of Ref. 31), the interatomic distances characterizing the Fe-As unit and the vertical distance of As with respect to the basal Fe plane are given by

$$d_{\text{Fe-Fe}} = \frac{a}{\sqrt{2}}, \quad d_{\text{Fe-As}} = \frac{a}{2\cos\theta},$$

$$d_v = \frac{a}{2}\tan\theta = c\left[z(\text{As}) - \frac{1}{2}\right]. \tag{1}$$

In order to investigate the dependence of the bandwidth on these structural parameters, we performed the following studies, which can be viewed as "numerical experiments:"

(i) Keeping the lattice constants a and c at their experimental values in undoped LaFeAsO, we studied how the band structure evolves as As is brought into the plane, starting from its experimental position down to a value comparable to the height of P in the LaFePO compound, i.e., reducing d_v or z(As) (hence decreasing θ and increasing θ_3). The resulting changes in the low-energy electronic structure corresponding to these calculations have been reported above in Sec. IV.

(ii) Keeping constant the Fe-As distance $d_{\text{Fe-As}} = 2.407$ Å (as well as c at the same value than above), we reduce the lattice parameter a. In doing so, the vertical distance d_v separating As from the Fe plane increases, resulting in a larger angle θ with the basal plane and a smaller angle at the summit θ_3.

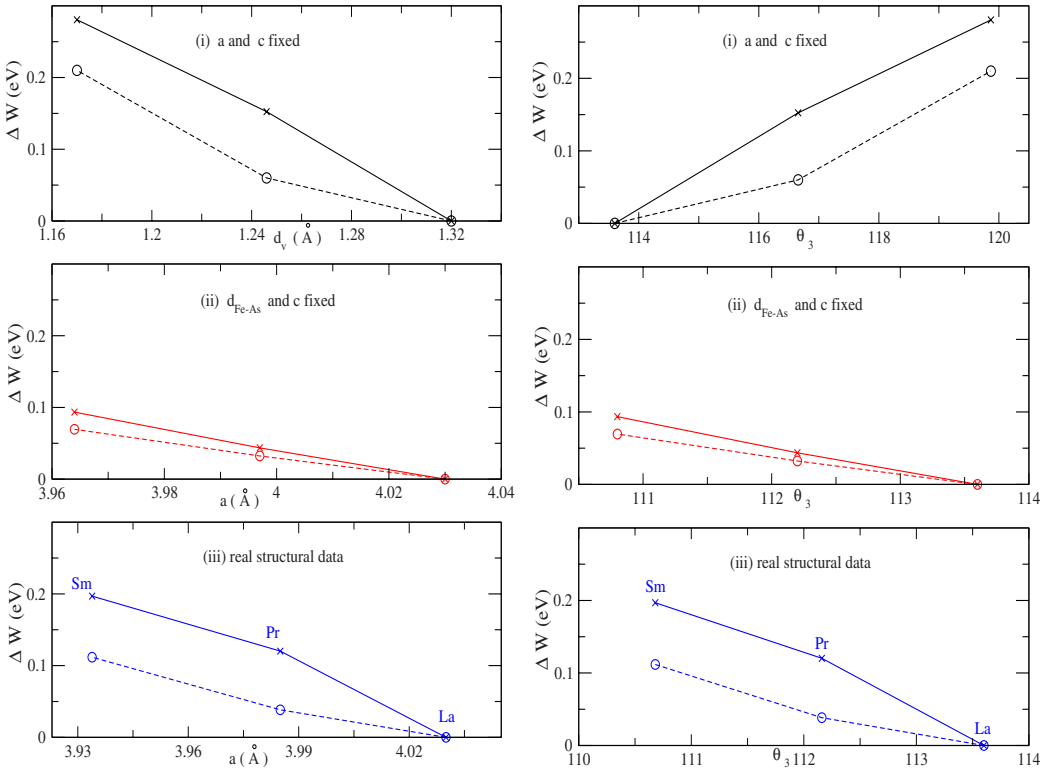

FIG. 9. (Color online) The change ΔW in the Fe $3d$ full bandwidth W (solid line) and the bandwidth of its occupied part W_{occ} (dashed line) with respect to the calculated value for LaFeAsO at its experimental structure (Ref. 7). These reference values are 4.25 eV for W and 1.95 eV for W_{occ}. From the top to bottom panels, we display the results for calculations (i)–(iii) as explained in the text. Left: ΔW as a function of d_v or a, as indicated. Right: ΔW as a function of θ_3. The structural data for Pr and Sm compounds were taken from Refs. 32 and 33, respectively.

(iii) Finally, we consider the actual experimental structure of the parent compounds LaFeAsO, PrFeAsO, and SmFeAsO. These three materials have almost identical Fe-As distances and correspond to decreasing values of a, similar to (ii). However in contrast to this case, they also correspond to decreasing values of the lattice constant c, with the REO unit getting closer to the FeAs one.

The results of these investigations are depicted in Fig. 9, in which we display the change in both the full bandwidth W of the Fe bands and the bandwidth of the occupied Fe states W_{occ} (i.e., the distance from the bottom of the Fe bands up to Fermi level). Both quantities provide useful information, but the latter is usually a better assessment of the relative importance of correlation effects (being related to the typical kinetic energy).

We note the following trends for the three numerical experiments above:

(i) As d_v is reduced for fixed a, a systematic increase in the bandwidth (and of the bandwidth of the occupied states) is observed. This is indeed expected: The direct Fe-Fe hopping is unchanged, while hybridization effects with As are increased as d_v is decreased, hence increasing the hopping through As sites. Thus, in this case, the bandwidth *decreases* as θ_3 decreases (and θ increases).

(ii) In the case where $d_{\mathrm{Fe\text{-}As}}$ is kept constant, both the occupied and the full bandwidths show a smaller effect as the a parameter decreases. Hence, there is a slight dependence of the bandwidth on the angles θ and θ_3 as compared to (i). The reason for this is that the increased Fe-Fe hopping (due to the decrease in a) is precisely compensated for by the decrease in indirect hopping through As (due to the increase in d_v).

(iii) Finally, for the real materials which also have basically a constant $d_{\mathrm{Fe\text{-}As}}$, we observe nevertheless a stronger *increase* in the bandwidth as a is reduced as compared to (ii). The reason for the difference with (ii) is that the lattice parameter c simultaneously decreases. Indeed the increase in the bandwidth comes also from unoccupied bands above Fermi level, reflecting the influence of the RE-O unit becoming closer. Hence, for the three materials investigated, the bandwidth *increases* as θ_3 decreases (and θ increases), in contrast to (i). The *occupied* bandwidth is even less sensitive to θ_3, again because of the compensating effect observed for (ii).

The general conclusion of this investigation is that, as expected physically, the bandwidth is controlled both by the direct Fe-Fe hopping in the plane and by the indirect hopping through As (in view of covalency and hybridization effects). Both the parameters a and θ (or θ_3) are therefore important. The bandwidth can in principle behave differently (increase or decrease) as the opening angle θ_3 is decreased. For the three real materials that we have investigated, the bandwidth displays a sizable *increase* for decreasing θ_3 however, in contradiction to the proposal made in Ref. 31. This increase is basically related to the decrease in the c parameter and the increase in Fe-Fe hopping (at constant c the bandwidth experiences a slighter effect).

VII. CONCLUSIONS

The compounds of the iron oxypnictide family share a similar overall electronic structure. Some important aspects, however, depend very sensitively on small structural changes, particularly on changes in interatomic distances and bond angles within the iron-pnictide plane. Using first-principles full-potential electronic structure calculations, we investigate this sensitive dependence, contrasting in particular LaFeAsO and LaFePO, which display different transport, magnetic, and superconducting properties. The width of the Fe bands is significantly larger for LaFePO, indicating a better metal and weaker electronic correlations. These two materials also present significant differences in their very low–energy band structure when calculations are performed at their experimental crystal structure. Both materials have three hole pockets around the Γ point and two electron pockets around the M point. However, one of the hole pockets changes from a three-dimensional one to a tube with two-dimensional dispersion when going from LaFePO to LaFeAsO. These differences are due to the shorter Fe-Fe distance and to the shorter distance of the pnictide to the iron plane in LaFePO. We have shown that the low-energy band structure of LaFeAsO evolves toward that of LaFePO as the As atom is lowered from its experimental position to a position closer to the Fe plane. We argue that the physical origin of this sensitivity to the iron-pnictide distance is the covalency of the iron-pnictide bond, leading to strong hybridization effects. To illustrate this, we have constructed Wannier functions, which are found to have a large spatial extension when restricting the energy window to the bands with dominant iron character. Finally, we have clarified how the bandwidth changes as one moves along the rare-earth series in REFeAsO. Since the Fe-As distance remains essentially constant, the Fe-Fe distance contracts, while the vertical distance to the Fe plane increases, resulting in a compensating effect and rather small changes of the bandwidth. A slight increase in the bandwidth of unoccupied states is observed, which is actually associated with the decreasing distance between the Fe-As and RE-O planes.

ACKNOWLEDGMENTS

This work was supported by the French ANR under project ETSF and a computing grant at IDRIS, Orsay (Project No. 081393). We acknowledge useful discussions with J. Bobroff, K. Nakamura, and S. Ishibashi.

[1] Y. Kamihara, T. Watanabe, M. Hirano, and H. Hosono, J. Am. Chem. Soc. **130**, 3296 (2008).
[2] K. Haule, J. H. Shim, and G. Kotliar, Phys. Rev. Lett. **100**, 226402 (2008).
[3] I. I. Mazin, D. J. Singh, M. D. Johannes, and M. H. Du, Phys. Rev. Lett. **101**, 057003 (2008).
[4] V. Cvetkovic and Z. Tesanovic, arXiv:0804.4678 (unpublished).
[5] D. Johnson and W. Jeitschko, J. Solid State Chem. **11**, 161 (1974).
[6] J. P. Carlo, Y. J. Uemura, T. Goko, G. J. MacDougall, J. A. Rodriguez, W. Yu, G. M. Luke, Pengcheng Dai, N. Shannon, S. Miyasaka, S. Suzuki, S. Tajima, G. F. Chen, W. Z. Hu, J. L. Luo, and N. L. Wang, arXiv:0805.2186 (unpublished).
[7] C. de la Cruz, Q. Huang, J. W. Lynn, J. Li, W. Ratcliff II, J. L. Zaretsky, H. A. Mook, G. F. Chen, J. L. Luo, N. L. Wang, and P. Dai, Nature (London) **453**, 899 (2008).
[8] Y. Kamihara, M. Hirano, H. Yanagi, T. Kamiya, Y. Saitoh, E. Ikenaga, K. Kobayashi, and H. Hosono, Phys. Rev. B **77**, 214515 (2008).
[9] Y. Kamihara, H. Hiramatsu, M. Hirano, R. Kawamura, H. Yanagi, T. Kamiya, and H. Hosono, J. Am. Chem. Soc. **128**, 10012 (2006).
[10] T. M. McQueen, M. Regulacio, A. J. Williams, Q. Huang, J. W. Lynn, Y. S. Hor, D. V. West, M. A. Green, and R. J. Cava, Phys. Rev. B **78**, 024521 (2008).
[11] S. Lebègue, Phys. Rev. B **75**, 035110 (2007).
[12] L. Boeri, O. V. Dolgov, and A. A. Golubov, Phys. Rev. Lett. **101**, 026403 (2008).
[13] D. J. Singh and M. H. Du, Phys. Rev. Lett. **100**, 237003 (2008).
[14] I. I. Mazin, M. D. Johannes, L. Boeri, K. Koepernik, and D. J. Singh, arXiv:0806.1869 (unpublished).
[15] F. Ma and Z. Y. Lu, Phys. Rev. B **78**, 033111 (2008).
[16] J. Dong, H. J. Zhang, G. Xu, Z. Li, G. Li, W. Z. Hu, D. Wu, G. F. Chen, X. Dai, J. L. Luo, Z. Fang, and N. L. Wang, Europhys. Lett. **83**, 27006 (2008).
[17] Z. P. Yin, S. Lebègue, M. J. Han, B. P. Neal, S. Y. Savrasov, and W. E. Pickett, Phys. Rev. Lett. **101**, 047001 (2008).
[18] P. Blaha, K. Schwarz, G. K. H. Madsen, D. Kvasnicka, and J. Luitz, *WIEN2K, An Augmented Planewave Plus Local Orbitals Program for Calculating Crystal Properties* (Technische Universitat Wien, Austria, 2002), http://www.wien2k.at.
[19] J. P. Perdew and Y. Wang, Phys. Rev. B **45**, 13244 (1992).
[20] J. P. Perdew, K. Burke, and M. Ernzerhof, Phys. Rev. Lett. **77**, 3865 (1996).
[21] S. Baroni, A. Dal Corso, S. de Gironcoli, P. Giannozzi, C. Cavazzoni, G. Ballabio, S. Scandolo, G. Chiarotti, P. Focher, A. Pasquarello, K. Laasonen, A. Trave, R. Car, N. Marzari, and A. Kokalj (http://www.quantum-espresso.org).
[22] K. Kuroki, S. Onari, R. Arita, H. Usui, Y. Tanaka, H. Kontani, and H. Aoki, arXiv:0803.3325, Phys. Rev. Lett. (to be published).
[23] N. Marzari and D. Vanderbilt, Phys. Rev. B **56**, 12847 (1997).
[24] http://www.wannier.org
[25] O. K. Andersen and T. Saha-Dasgupta, Phys. Rev. B **62**, R16219 (2000).
[26] S. Ishibashi, K. Terakura, and H. Hosono, J. Phys. Soc. Jpn. **77**, 053709 (2008).
[27] D. H. Lu, M. Yi, S.-K. Mo, A. S. Erickson, J. Analytis, J.-H. Chu, D. J. Singh, Z. Hussain, T. H. Geballe, I. R. Fisher, and Z.-X. Shen, arXiv:0807.2009 (unpublished).
[28] O. K. Andersen and O. Jepsen, Phys. Rev. Lett. **53**, 2571 (1984).
[29] F. Lechermann, A. Georges, A. Poteryaev, S. Biermann, M. Posternak, A. Yamasaki, and O. K. Andersen, Phys. Rev. B **74**, 125120 (2006).

[30] A. O. Shorikov, M. A. Korotin, S. V. Streltsov, S. L. Skornyakov, D. M. Korotin, and V. I. Anisimov, arXiv:0804.3283 (unpublished).
[31] J. Zhao, Q. Huang, C. de la Cruz, Sh. Li, J. W. Lynn, Y. Chen, M. A. Green, G. F. Chen, G. Li, Z. Li, J. L. Luo, N. L. Wang, and P. Dai, arXiv:0806.2528 (unpublished).
[32] P. Quebe, L. J. Terböchte, and W. Jeitschko, J. Alloys Compd. **302**, 70 (2000).
[33] N. D. Zhigadlo, S. Katrych, Z. Bukowski, and J. Karpinski, arXiv:0806.0337 (unpublished).